Enhanced Properties of Innovative Laponite-Filled Waterborne Acrylic Resin Dispersions

M. L. Nobel, E. Mendes, S. J. Picken

Polymer Materials and Engineering, Faculty of Applied Sciences, Delft University of Technology, Julianalaan 136, 2628 BL Delft, The Netherlands

Received 23 February 2006; accepted 6 April 2006
DOI 10.1002/app.24608
Published online in Wiley InterScience (www.interscience.wiley.com).

ABSTRACT: In view of the possible future applications of waterborne automotive coatings, acrylic-based nanocomposite dispersions were investigated by the simple mixing of aqueous laponite nanoparticle dispersions with acrylic resin dispersions. The mechanical, flow, and leveling properties of waterborne nanocomposite dispersion formulations containing increasing concentrations of silicate and nonvolatile components (nvc) in the acrylic dispersions were investigated. The results obtained were related to the morphological information obtained from transmission electron microscopy and wide-angle X-ray scattering measurements in liquid suspension or on the cured films. At low synthetic silicate loading when flow, leveling, and appearance properties were still acceptable for processing and application, a large increase in the modulus of the cured coating films was observed, which was a result of the special morphology of the laponite-rich regions of the cured film. © 2006 Wiley Periodicals, Inc. J Appl Polym Sci 103: 687–697, 2007

Key words: resins; nanocomposites; clay

INTRODUCTION

Nanostructured composites containing montmorillonite-type silicate layers embedded in various polymer matrices have been intensively studied in recent years. Such inorganic filler particles can also be added to polymer dispersions, as used for waterborne coatings to improve mechanical properties. In addition, properties such as color, flame resistance, and permeability may be influenced. This topic has recently drawn increased attention because of environmental regulations that will be applied to procedures in automotive production, where the use of solvent-based coating systems is under increasing pressure. The growing need for more environmentally friendly alternatives such as solvent-free lacquer systems has increased the interest in waterborne (WB) systems. These contain substantially less solvent and are easy to produce. A disadvantage is that until now they have contained components that are far more expensive than the components of solvent-based systems. Moreover, it is harder (and therefore more expensive) to obtain the same product quality as solvent-borne coating systems. The practical aim of our research was the development of an innovative technology for waterborne nanoparticle resin systems, yielding automotive coatings with a superior mix of material and application properties.[1] The desired improvements included scratch resistance, resistance to chemical degradation, and improved mechanical properties, which could result from the synergistic effect of the organic and inorganic components. The effects of different nanoparticles on the properties of polymers vary a lot depending on the system, so this requires more detailed analysis. In previous research we explored an acrylic oligomer in an organic solvent resin system with incorporated Cloisite 30B (C30B), aiming to understand how the addition of large-aspect-ratio montmorillonite platelets influences the organic resin matrix in structural and performance terms.[2] In the present study, smaller-sized synthetic laponite disks were added to the water phase of an acrylic resin dispersion in order to study the structure of the nanoparticle/water/resin particle mixture as a function of concentration. We focused on the morphology of the nanocomposites and its effect on the flow properties of the acrylic dispersion particles in the uncured resin state. The results were combined with analysis of the mechanical properties of acrylic films formed after a process of curing the nanoparticles containing acrylic dispersions.

Correspondence to: S. J. Picken (Picken@tnw.tudelft.nl).
Contract grant sponsor: Dutch Programme EET (Economy, Ecology, Technology), a joint initiative of the Ministries of Economic Affairs, Education, Culture and Sciences and of Housing, Spatial Planning and the Environment, run by the EET Programme Office, a partnership of Senter and Novem.

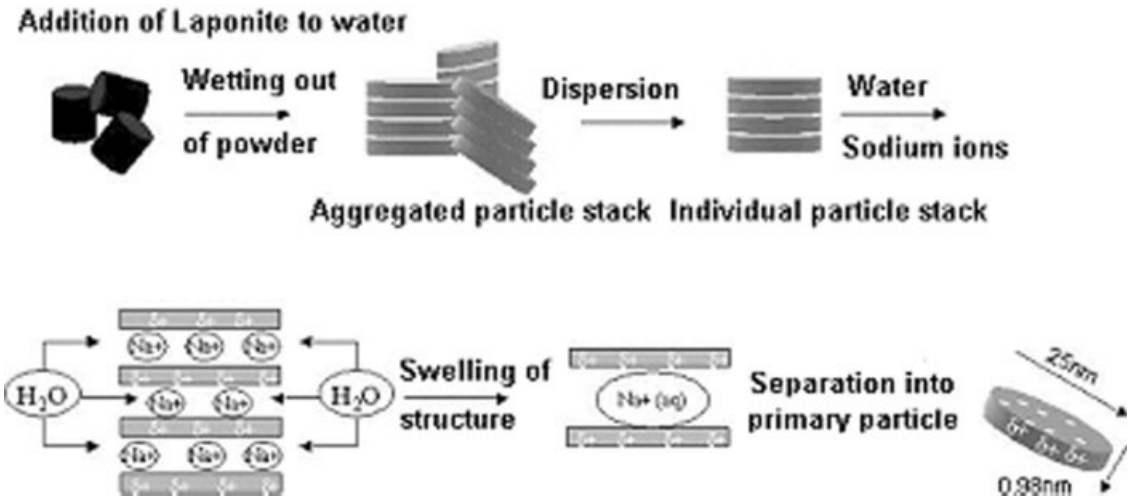

Scheme 1 Laponite dispersion process in water.

EXPERIMENTAL

Materials

Suspensions of natural colloidal magnesium–silicate platelets exhibit a wide range of structural and mechanical properties and are frequently used as thickeners, fillers, and antisettling agents. Montmorillonite, as used in previous studies,[2] is one such natural clay. Primary particles are platelets or layers, each made up of two tetrahedral sheets sandwiching a central octahedral sheet. Multiple layers/platelets form tactoids or crystallites in which the negative charge is balanced by inter- and intralamellar sodium cations;[3] groups of tactoids form aggregates or agglomerates.

Montmorillonite platelets are between 200 nm and 1 μm in diameter. One disadvantage of natural clays compared to their synthetic counterparts is that they are usually very polydisperse in both shape and size. Synthetic clays comparatively have a much lower degree of polydispersity when in solution. Another disadvantage can be discoloration of the resulting nanocomposites based on natural clays. This is a result of either impurities within the crystal structure or dissociation of the functionalized chemicals necessary to promote exfoliation.

The synthetic layered silicate (SLS) used in the preparation of the waterborne polyacrylate nanocomposite coatings was supplied by Rockwood Additives Ltd. (Cheshire, UK) under the trade name Laponite RD. Primary laponite particles are only 25 nm across and 1 nm thick. Laponite platelets are usually stacked in aggregates, in which clay sheets are separated by exchangeable cations and one or two water layers. Each layer comprises three sheets, two outer tetrahedral silica sheets and a central octahedral magnesium sheet. Part of the magnesium in the central sheet is replaced by lithium, resulting in a net negative charge of the layer. This is balanced by sodium ions located between adjacent layers in a stack. The empirical formula of the laponite structure is $Na^{+}_{0.7}\,[(Si_8\,Mg_{5.5}\,Li_{0.3})\,O_{20}(OH)_4]^{-0.7}$.[4]

The process of dispersing laponite from powder to individual particles is shown in Scheme 1.

The powder was wetted out in an aqueous environment under moderate shearing using a high-speed disperser (2000 rpm). The aggregated particle stacks were dispersed into primary particle stacks when the speed was raised to 6000 rpm. This rotation speed was maintained for 1 h.

The stability of laponite in a water dispersion decreases with time. According to particle size measurement over time, which was performed by the supplier, sol formation is stable as long as 90 days when a maximum concentration of laponite particles of 15% (w/w) is not exceeded.[4] Decreasing of sol stability occurs more rapidly than the aging of the laponite particles themselves (because of the release of Mg^{2+} ions), which occurs on a time scale of hundreds of days.[5,6] For this reason, coating formulations using laponite dispersions have been based on a 4% (w/w) laponite content of the stock solution. Dispersion samples formulated with laponite dispersions were investigated within several weeks of preparation, which is within the stability window specified by the manufacturer at room temperature.[4] At a pH < 9, Laponite RD particles dissolve because of magnesium dissociation, whereas at a pH > 10, silica dissolution occurs.[7] The particles are stable at a pH between 9 and 9.5; therefore, the solutions were prepared under these alkaline conditions, which is also a suitable range for maintaining stability of the polymer dispersion.

A one-component (1K) self-crosslinkable dispersion formulation was selected in which the addition

TABLE I
Characteristics of All-Acrylic Dispersion Formulation, Setalux 6768

Description	
Acrylic polymer–stabilized acrylate dispersion in demineralized water with a core–shell structure consisting of a hydrophobic core and a hydrophilic shell.	
Characteristic	
Nonvolatile	39%–41%
MFT	7°C
pH	7–9
Density	1.04 kg/dm^3
T_g core	±125°C
T_g shell	±40°C
Appearance	Clear

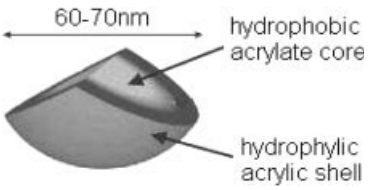

of laponite particles to the water phase could be studied. These 1K self-crosslinkable systems have no pot-life problems. They do not need the addition of a crosslinking agent prior to application. Nuplex Resins (formerly Akzo Nobel Resins) provided Setalux 6768, a specialty acrylic dispersion (see Table I). Setalux 6768 acrylic dispersion is stabilized by electrostatic repulsion of the anionic resin particles. It was originally developed for topcoats in the general metal market and at the moment is finding many applications on other substrates such as wood and plastic. Upon drying, the crosslinking mechanism is triggered, resulting in a fully cured coating.

Compounding and preparation of all acrylic nanocomposite dispersions

The synthetic route of choice for making a nanocomposite depends on whether the final material is required as an intercalated or exfoliated system. With an intercalate, the organic component is inserted between the disks of laponite such that the interdisk spacing is an expanded, well-defined spatial distance. In an exfoliated structure, the laponite disks are completely separated, and the individual silicate disks are distributed throughout the organic matrix. A third alternative is dispersion of the laponite powder particles (tactoids) within the polymer matrix, but this simply represents use of laponite as a conventional filler. With polymer–clay systems, the correct selection of modified clay is essential to ensure effective penetration of the polymer or its precursor into the interlayer spacing of the clay so as to obtain the desired exfoliated or intercalated product. However, laponite disks spontaneously disperse in water aided by low shear and are therefore in an exfoliated state when the dispersion is mixed with the WBAA polymer dispersion. During the dispersing of the laponite disks, water molecules penetrate between the layers of individual laponite particles where the sodium ions are located. This causes the structure to swell. Electrostatic attractions draw the sodium ions in solution toward the crystal surface, and osmotic pressure from the bulk of water pulls them away. An equilibrium is established where the sodium ions are held in a diffuse region on both sides of the dispersed laponite crystal. These are known as electrical double layers. When two particles approach, positive charges of the electrical double layer and positive charges on the edges of the disks repel each other, thereby stabilizing the exfoliated state. A dispersion of exfoliated laponite particles from a sol-forming grade exhibits low viscosity and a Newtonian rheology.[4]

Reagglomeration of the laponite/water suspension can occur when the compatibility of the laponite platelets with the WBAA polymer dispersion is insufficient. Laponite disks in suspension can be incorporated either by simple mixing with the WBAA polymer dispersion itself, as described is this article, or via mixing with chemically similar polymeric precursors, which are postemulsified to give the corresponding laponite–polymer nanocomposite dispersions. In the first case, the laponite disks are in the water phase of the polymer dispersions. The latter procedure will presumably yield laponite disks inside the polymer droplets. Such a system will be described in future articles. In addition to the anticipated effects on the rheology of the different morphologies, it is expected that the film formation of the dispersions and thus the resulting mechanical properties of the cured films will be influenced. Figure 1 gives an overview of the processes that occur upon film formation of a dispersion.

Setalux 6768 consists of particles of approximately 60–70 nm in diameter. During the film formation six processes occur that can be grouped into three stages. In total, the dispersion changes from a heterogeneous polymer in water dispersion into a transparent homogenous film. During water evaporation and

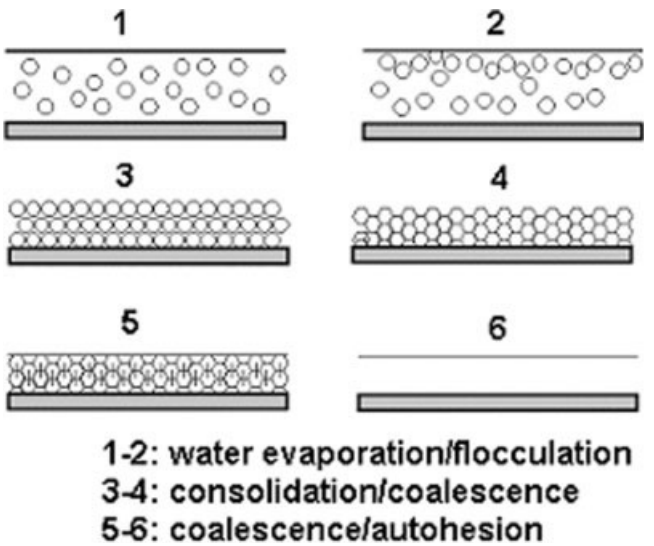

Figure 1 Film formation process of waterborne dispersions.

flocculation (see processes 1 and 2 in Fig. 1), external factors like air speed, relative humidity, and temperature of the environment influence drying. There is a balance between the kinetics of drying and the kinetics of fusion of the particles (coalescence). Therefore, water evaporation followed by consolidation and fusion of the particles (processes 1–2 and 3–4 in Fig. 3) can happen at the same time, where the balance between attraction and repulsion forces determines the local time stability. Particles in the nanometer range have huge attractive forces, and repulsion must be gained through electrostatic interactions because of charges on the particle surface. These charges are compensated by counterions in solution, and an electrical double layer is formed. During drying the electrolyte concentration increases, causing the double layer to shrink, and the dispersion becomes less stable. For the best hexagonal packing during coalescence, it is important that the particles stay stable as long as possible. During the deformation stage (i.e., consolidation), particle boundaries are still present. The presence of water is crucial for coalescence because during the last stage of the film formation, the particles lose their identity, and the polymer chains from different particles become entangled. During this process the film obtains its final strength, which can take several weeks.[8]

The polyacrylate nanocomposite dispersions and films were prepared as described in Scheme 2.

Laponite was dispersed to 4% (w/w) in demineralized water according to Scheme 1. At this point, the laponite particles were separated into individual platelets.

To make them more compatible with the acrylic resin particles, a small amount (1% of particle weight) of a phosphonic ester (Phospholan PNP9, Akzo Nobel surfactant) was added. This anionic phosphate ester (see Table II) attached to the edges of the laponite disks. The nonylphenol/ethanol groups of the phosphate ester caused a slight increase in the hydrophobicity of the disks. Dispersing continued at 2000 rpm under ultrasonification, at which the temperature of the laponite solution rose to 65°C because of shear. After 4h the prepared organomodified laponite solution was added to the Setalux 6768 dispersion by simple manual mixing. Nanocomposite dispersions containing 2%–12% (w/w) laponite particles relative to the polymer were prepared.

The relationship between the weight percentage of the laponite and the volume fraction (V_{fL}) of the laponite can be calculated using eq. (1):

$$V_{fL} = \frac{w_L {\rho_L}^{-1}}{w_L {\rho_L}^{-1} + (1 - w_L){\rho_s}^{-1}} \quad \text{with: } \rho_L = 2.65 \text{ g/cm}^3 \text{ and } \rho_s = 0.998 \text{ g/cm}^3 \quad (1)$$

where ρ_L is 2.65 g/cm^3 and ρ_s is 0.998 g/cm^3.

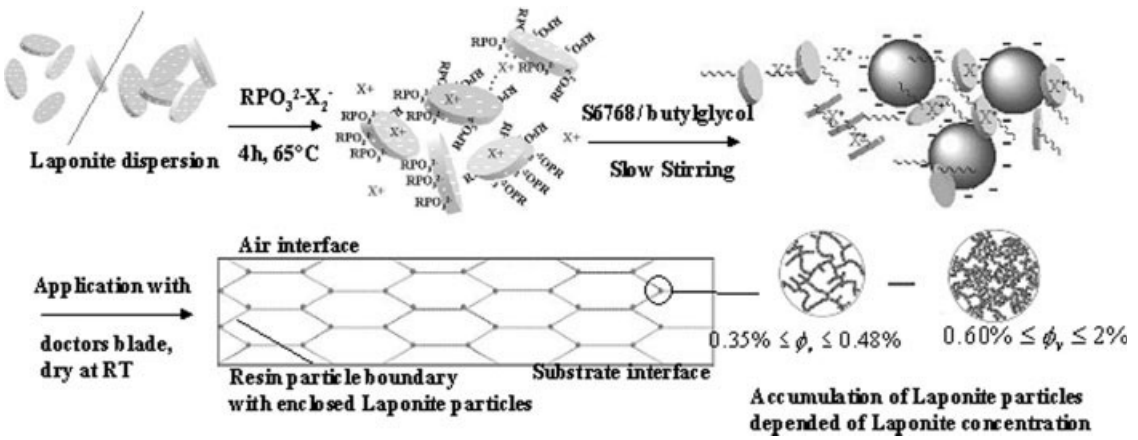

Scheme 2 Scheme of nanocomposite preparation.

TABLE II
General Structure of Phosphate Ester, Phospholan PNP9

Phospholan PNP9
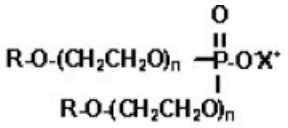
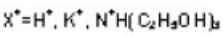
Hydrophobic part: Nonylphenol, EO 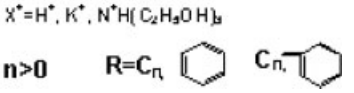

For example, 4% (w/w) laponite upon an nvc content of the dispersion contains 0.0161 V_{fL} laponite disks in the cured coating film.

The relationship between the weight percentage of solid resin in the dispersion and the volume fraction of solid resin in the dispersion can be calculated using eq. (2):

$$V_{fR} = \frac{w_{\text{resin}}\rho_{\text{resin}}^{-1}}{w_{\text{resin}}\rho_{\text{resin}}^{-1} + (1 - w_{\text{resin}})\rho_{\text{water}}^{-1}} \quad (2)$$

where ρ_{resin} is 1.04 g/cm^3 and ρ_{water} is 0.998 g/cm^3.

For example, 40% (w/w) nvc of the dispersion contains a volume fraction of 0.397 of solid resin in the dispersion.

EXPERIMENTAL

Transmission electron microscopy

Transmission electron microscopy (TEM) was performed using a Philips CM30T electron microscope with a LaB_6 filament operated at 300 kV. Ultramicrotomed slices of the samples, supported by a cured dispersion, were placed on a copper grid. Four cured acrylic films with varying laponite concentrations in the range of 2%–8% (w/w) clay platelets were studied using this technique.

Dynamic mechanical thermal analysis

Dynamic mechanical thermal measurements (DMTA) were carried out using a modified Rheovibron (Toyo Baldwin, type DDV-II-C) at a frequency of 11 Hz with a dynamic strain of 0.03%. The temperature was varied between −50°C and 200°C at a heating rate of 5°C/min.

To keep the sample sufficiently loaded during the experiment (to keep the sample flat), a static force was applied to the sample. As the stiffness of the sample changed with temperature, the static force level was adjusted at each temperature. In the glassy state and in the glass-transition temperature region, static stress was set at five times the dynamic stress as results from the applied dynamic strain of 0.03%.

In the rubber region, a constant static stress, typically 0.4 MPa, was applied to the sample.

The samples were punched from a freestanding film of the coating using a special cutting device placed in a press. The clamped samples in the test geometry were 3 mm in width and 30 mm in length.

The thickness of a sample was determined using a inductive thickness gauge (Isoscope® MP, Fischer Instrumentation). The thickness was determined at at least five spots on the sample, and the average thickness and the standard deviation were determined. The average thickness for all samples was approximately 50 μm. Variation in sample thickness, roughly 2–10 μm, was taken into account during the processing of the results.

All measurements were done in tensile mode, and at each temperature the tensile storage modulus, E', the tensile loss modulus, E'', and the tan δ, tan $\delta = E''/E'$, were determined.[9]

Thermogravimetric analysis

The exact amount of volatile components in the composite samples was determined using thermogravimetric analysis (TGA). The samples were heated from 25°C to 120°C at a rate of 25°C/min and were kept at this temperature for 30 min. Because acrylic resin and laponite were the only residues, the nonvolatile component content of our compositions could be calculated as that which remained. The amount of weight loss as observed by TGA of the pure laponite and acrylic resin was taken into account in this measurement.

DMA rheology

The rheological experiments were conducted on a controlled strain Rheometrics Ares rheometer equipped with a Couette geometry. The bob and cup were 31.97 and 33.9 mm in diameter, respectively. The length of the bob was 33.35 mm. Steady-shear-rate transient and oscillatory measurements were performed in order to study the rheological behavior of filled acrylic polymer solutions containing varying concentrations of filler. All measurements were performed at room temperature.

X-ray diffraction

A Bruker-Nonius D8-Discover setup with a 2-D detector was used to perform the experiments. The sample to detector distance was set to 10 cm, and the incident beam wavelength was 1.54 Å. Special attention was paid to sample preparation: the dispersions were measured in a capillary to ensure a constant thickness and random orientation. Cured films were prepared in the absence of surface defects and at an overall thickness of 0.652 mm.

RESULTS AND DISCUSSION

Analyzing polymer nanocomposite X-ray scattering

Laponite particle stacks consisted of individual layers about 0.98 nm thick with a radius between 20 and 30 nm. Decreasing the mean stack size and increasing the fraction of individual layers broadened the reflections, as well as decreasing the magnitude of $I(q \rightarrow 0)$, which was proportional to the average stack size.

Completely suspended clay scattered strongly at low q, where the scattering vector was $q = 4\pi[\sin(\theta)/\lambda]$.[10] Regardless of the layer composition, the structure factor increased markedly at low angles.

The power-law dependence of $I(q)$ at a low q approached a slope of -2 for highly dispersed thin plates. Scaling behavior in this regime for layered stacks was substantially less ($I \approx q^m$, $m \leq -2$). At a high q (thickness of platelets $\sim$ 1 nm), the use of the complete expression for the form factor of an (infinite) plate rather than the thin-plate approximation was required to correctly interpret the relative magnitudes of the reflections.[7]

Figure 2(a) summarizes representative data sets for amorphous scattering of the unfilled dispersion film, laponite powder patterns, and acrylic nanocomposite films with dispersed laponite at increasing concentrations. The results are shown where the amorphous scattering of the unfilled S6768 dispersion sample has been subtracted. The scattering curves for films with increasing laponite concentration were similar, suggesting no significant structural changes occurred for concentrations from 2% to 8 % (w/w) laponite, although the shift in Figure 2(a) indicates less dispersion with increasing clay content. As the concentration of laponite increased, the scattering intensity increased for all q values of the cured films.

The laponite scattering at smaller angles revealed that the form factor (m) of the laponite disks [$I(q) \sim q^m$; see Fig. 2(b)] decreased with a shifting of the intensity of the increasing amount of laponite containing samples up, whereas the slopes of the curves increased. The power-law dependence of $I(q)$ at lower q values, below the first scattering peak, approached a slope of -2 for highly dispersed systems. The polymer nanocomposite sample containing the lowest filler concentration, 2% (w/w), had a slope of -2.4. The slope increased with a higher filler content, indicating an increase in stacking.

TEM analysis of cured films

TEM analysis of three cured nanocomposite films with increasing filler loading was performed. Figure 3 displays an overview of the obtained TEM results.

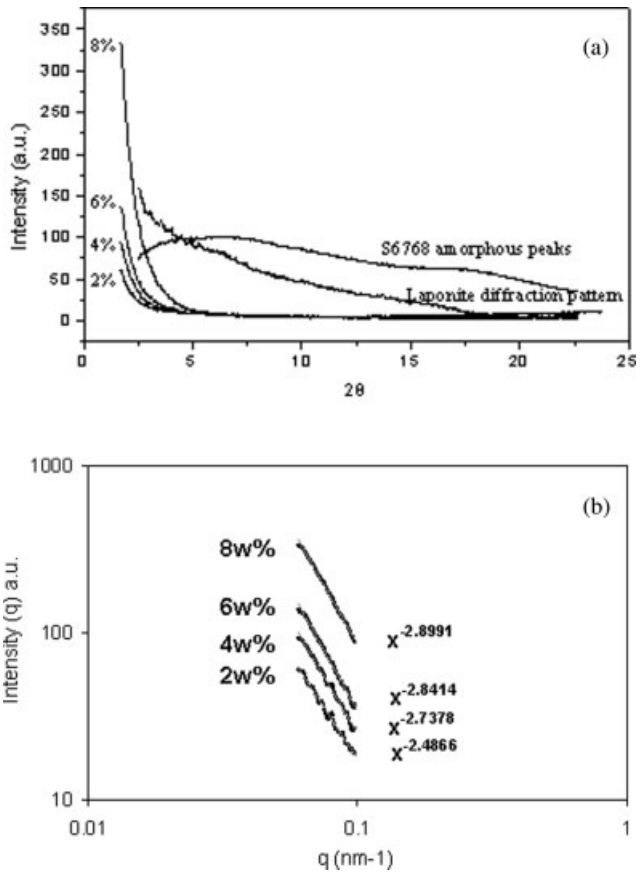

Figure 2 (a) X-ray diffraction data of 0%–8% (w/w) laponite particles containing cured dispersion. (b) Power law dependence at smaller angles of the diffraction data of 0%–8% (w/w) laponite particles containing cured dispersion.

At a silicate concentration of 2% (w/w) disks, the largest amount of individual silicate platelets could be observed, with a significant number oriented in the plane of the film. Overall, the structure was a mixture of single and stacked laponite disks, as can be seen in the magnified inset (B) of Figure 3(a). It is interesting to observe the accumulation of highly oriented laponite disks along the edge of the films [see upper magnification (A) in Fig. 3(a)], which confirmed the exclusion of the partially hydrophobic laponite particles away from the bulk of the film when the curing proceeded. At higher silicate loadings of 4% (w/w) disks, a further increase in stacking was observed in the bulk of the film away from the film surface [see magnification (A) of Fig. 3(b)]. This increase in stacking corresponded to the X-ray diffraction results described in the previous section. In contrast to samples containing 2% (w/w) laponite-filled S6768 films, some ''face''-oriented disks were observed, as shown in magnification (B) of Figure 3(b). The highest silicate loading, 8% (w/w) disks, showed that locally the laponite disks were arranged in cell-like structures, templated by the coalescence of the resin particles during film formation.

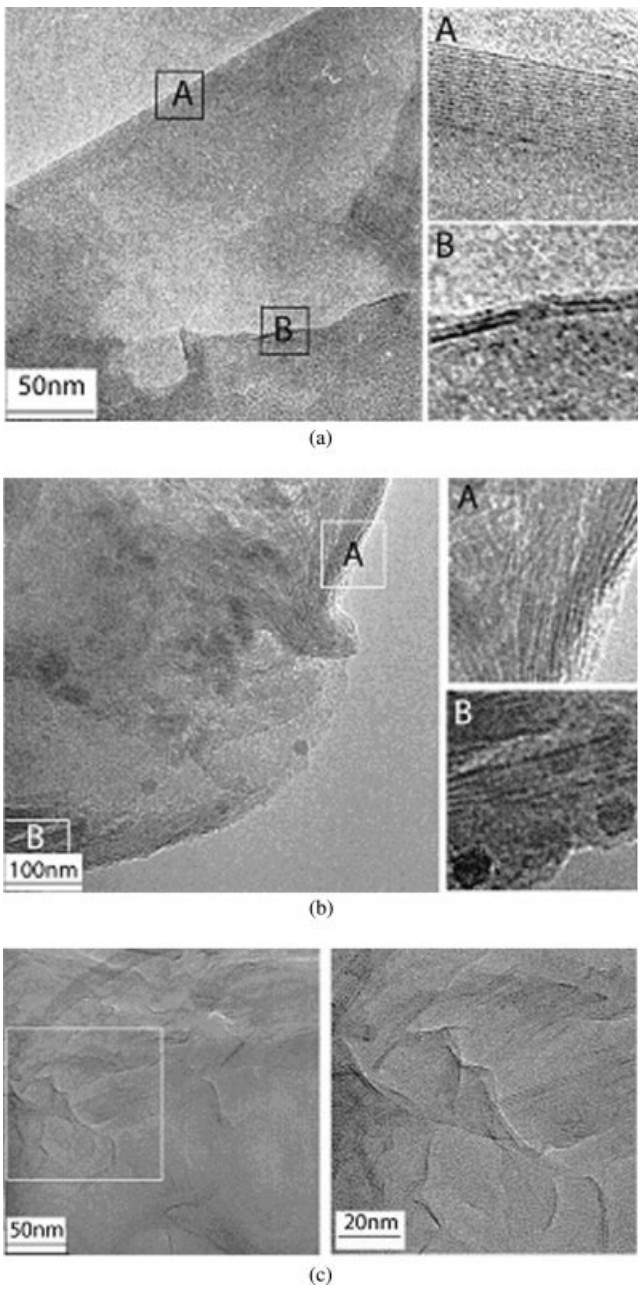

Figure 3 TEM photographs of nanocomposite dispersion films containing up to 8% (w/w) laponite particles: (a) 2% (w/w) laponite particles, (b) 4% (w/w) laponite particles, (c) 8% (w/w) laponite particles.

Rheological properties of nanocomposite dispersions by dynamic mechanical analysis

Laponite suspensions are used in a variety of industrial formulations, including paints, coatings, cosmetics, personal care products, household cleaners, and adhesives. In these applications, polymer additives are incorporated into the suspension as rheological modifiers or stabilizers. They are incorporated in order to utilize their gel-forming behavior as a thickening agent.

The mechanism of such a gel formation process is a subject of considerable debate. The two main hypotheses are repulsive gelation from overlapping double layers and aggregation because of attractive electrostatic interactions between disk edges and faces.[11–14]

For coatings based on water-based resins systems, which contain suspensions of nanosized laponite disks, observation and preferably control of the gelation behavior are important during the application. The rheological behavior of the dispersion system is influenced by the location of the laponite disks. When the nanoparticles are in the water phase of a dispersion, they would be expected to influence the rheology of the dispersion to a greater extent than when they are inside the resin particles. In future articles we will describe a composite state in which the nanoparticles are in the resin particles. When this is true, the nanoparticles could give rise to hindered coalescence during film formation by obstructing the fusion of the polymer particles via steric hindrance as well as the higher viscosity of the polymer particles as a result of the filler content.

According to the the C-P-OM model (Edwards and Bremner, 1967),[15] polyvalent cations are crucial to bridge clay and organic matter. Giovannini and Sequi (1978)[16] hypothesized that these cations serve as junctions in a net or mesh composed of polymeric chains of organic matter. When these cations are removed, this mesh is weakened at the junctions; thus, stability of the formed gellated structure decreases. Olivier and Pefferkorn[17] showed that mixing of aggregates with polymer induces ''swelling,'' which was attributed to the interpenetration of colliding aggregates and adsorption of polymer on the aggregate subunits. Below a critical volume fraction of 0.60%, these aggregates form bundles that give laponite particles combined with polymer a fibrous texture. Beyond this volume fraction the structure is more heterogeneous, with areas of varying particle density. Upon aging, rearrangement of the polymer bridges occurs, which induces dense packing of the disks.[18]

As a suspension in water, the laponite disks remained dispersed as individual disks so long as no significant amount of polyvalent cations were present. Visual inspection of up to 8% (w/w) of the laponite disks in water indicated little or no increase in viscosity. For the rheological measurements, nanocomposite dispersions containing an increasing amount of laponite and a fixed solid resin content (0.3 volume fraction) as well as nanocomposite dispersions containing an increasing amount of solid resin with a fixed amount of laponite disks, 6.5% (w/w), were prepared. This combination sample preparation provided information about the structure upon the addition of an increasing concentra-

tion of laponite disks in the water phase of the dispersion combined with the influence of a decreasing amount of nonvolatile resin. The mixtures were mixed for several minutes a day over 1 week. Good homogenization can be obtained using such mild shear conditions. Depending on the sample composition, liquidlike, elastic fluid, gel-like, or ''solid'' rubberlike behavior could be observed.

It was interesting to investigate polymer nanocomposite resin systems in which the amount of laponite particles was kept constant with respect to the solid resin weight while varying the amount of resin solids. As shown in Scheme 2, this meant not only that resin content varied but also that laponite content differed in each sample at a fixed weight ratio.

Oscillatory strain-dependent measurements at a frequency of 10 rad/s of dispersions containing a fixed amount of laponite disks, 6.5% (w/w), in the water phase mixed with the 0.397 V_{fR} nonvolatile component Setalux 6768 acrylic resin dispersion are shown in Figure 4(a). The addition of extra water or its evaporation yielded laponite-filled dispersions containing 0.169–0.514 V_{fR} solid resin particles in an aqueous environment. A broad linear region of all samples was observed, with the critical strain occurring for most samples between 10% and 15%.

Frequency-dependent oscillatory shear experiments at 10% strain are shown in Figure 4(b,c). A broad linear viscoelastic range and a frequency-independent storage modulus between 1×10^{-2} and 1×10^{3} Pa were observed over several decades in frequency. Because all samples showed a larger G' than G'', all filled concentrations showed solidlike concentrations, in contrast to the unfilled resin dispersion. where $G'' > G'$. The rise in modulus of the nanofilled dispersions made the dispersions suitable for paint formulation using a lower nonvolatile component concentration than usual. It should be mentioned that the more dilute concentrations of 0.169–0.27 V_{fR} solid resin are more susceptible to measurement errors because of water evaporation and low torque levels.

Figure 4(d) shows the viscosity curves as a function of shear rate. The unfilled dispersion showed Newtonian behavior over the complete range of shear rates. The addition of laponite disks introduced constant pseudoplastic behavior into the system. When the laponite particles interacted and

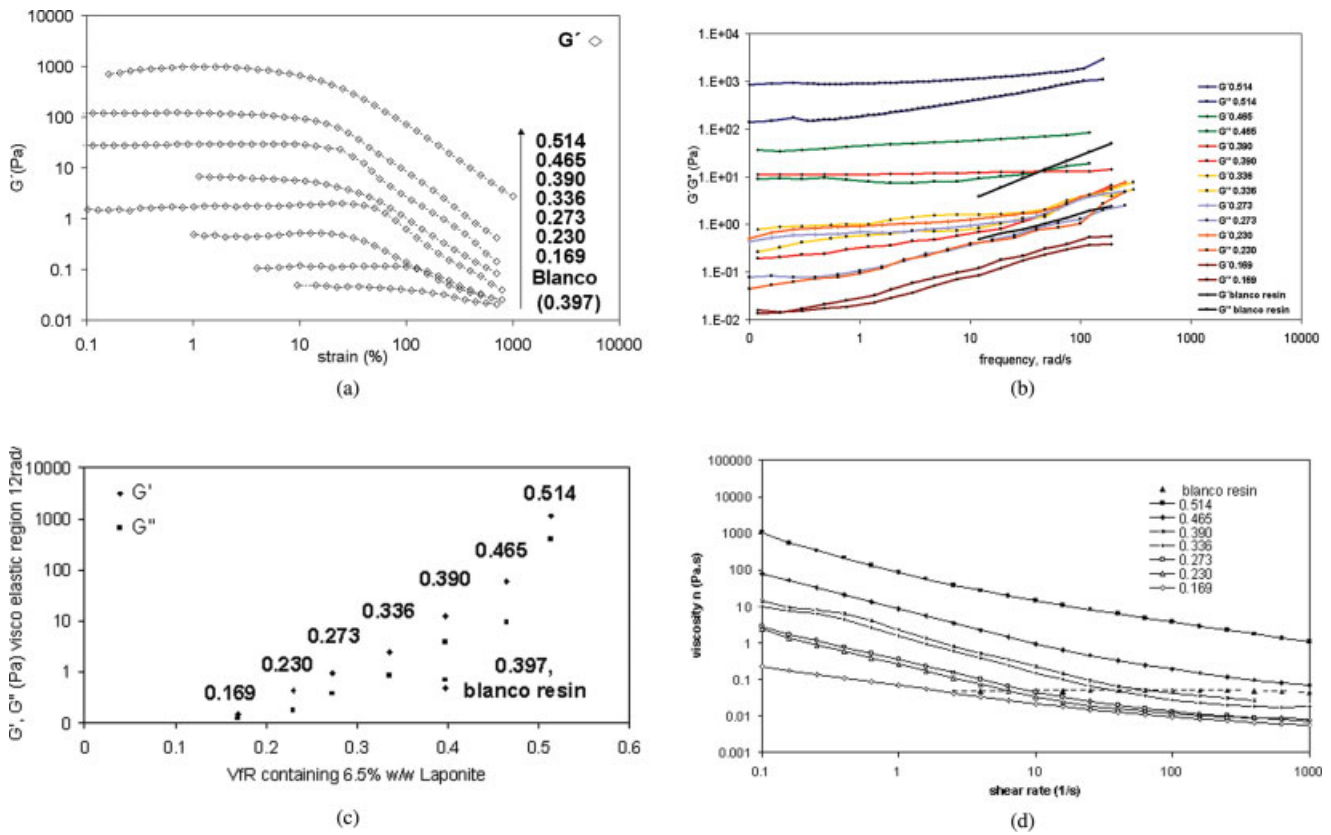

Figure 4 (a) Oscillatory strain–dependent data of 0.169–0.514 V_{fR} nvc dispersions containing 6.5% (w/w) laponite disks in the water phase of the dispersion. Measurements were performed at a frequency of 12 rad/s. (b) Oscillatory frequency–dependent data of the same material over a broad range of frequencies. Measurements were performed at a strain of 10%. (c) Increase in storage and loss modulus. (d) Flow curves of 0.169–0.514 V_{fR} nvc dispersions containing 6.5% (w/w) laponite disks in the water phase of the dispersion. [Color figure can be viewed in the online issue, which is available at www.interscience.wiley.com.]

formed three-dimensional aggregates, more filler content resulted in systems with higher pseudoplasticity. Because the amount of pseudoplasticity was nearly constant with increasing laponite content, it was expected that the laponite particles would interact preferentially with the resin particles, initially resulting in only higher viscosity. Viscosity increased by almost four decades when the concentration of resin was increased from 0.169 to 0.154 V_{fR}.

Within the viscoelastic region, frequency-dependent oscillatory shear measurements of the composite dispersions containing 0.302 V_{fR} dispersion filled with 6% and 12% (w/w) laponite disks, as shown in Figure 5(a), indicated an increase in both moduli as viscosity of half a decade combined with a similar degree of pseudoplasticity of the elastic solids.

The flow profile shown in Figure 5(b) indicates there was high viscosity at low shear stress, which could give rise to leveling problems during film formation. Leveling problems became even more serious at laponite concentrations at which a yield stress had developed [see Fig. 5(c), curves 6%–12% (w/w) laponite]. This behavior can be explained by the visualization of the laponite-filled emulsion shown in Scheme 2. Laponite aggregates will initially interact via loose connections in the water phase of the dispersion but as a polymer nanocomposite dispersion increases, networks and aggregates are formed. At higher laponite concentrations this results in both an increase in viscosity and the development of yield stress.

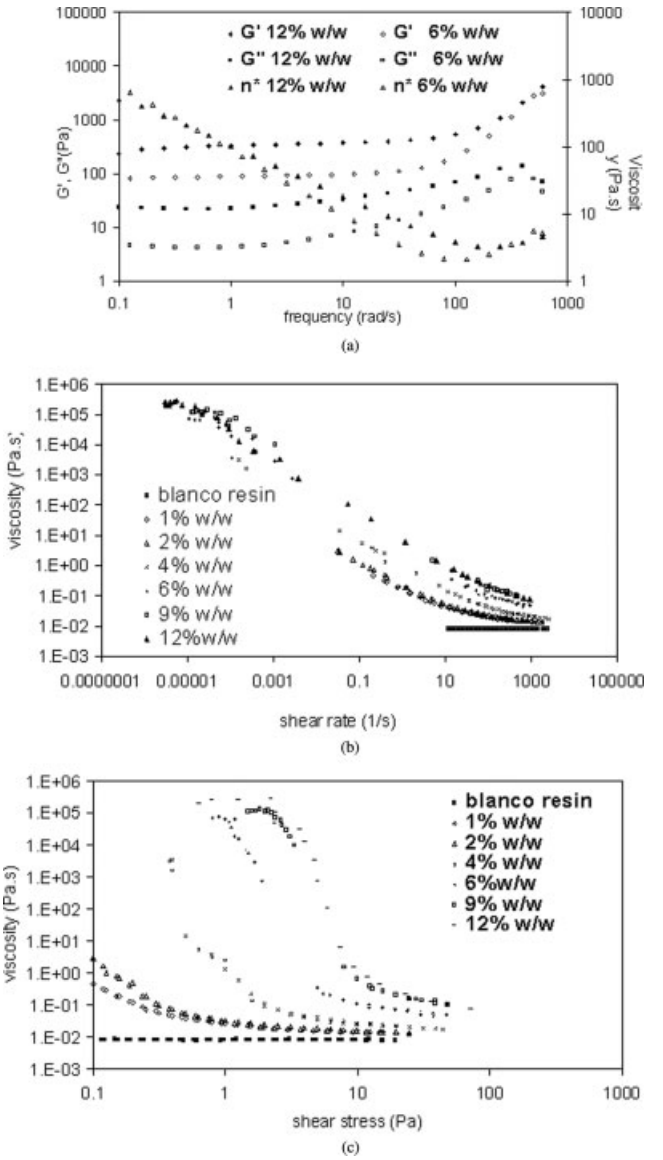

Figure 5 (a) Frequency-dependent curves at 10% strain of 0.302 V_{fR} nvc dispersions containing 6% and 12% (w/w) laponite particles. (b) Flow profile of 0.302 V_{fR} nvc dispersions containing up to 12% (w/w) laponite particles. (c) Viscosity as a function of shear stress of 0.302 V_{fR} nvc dispersions containing up to 12% (w/w) laponite particles.

Analysis of modulus of cured nanocomposite dispersions

The aspect ratio of the reinforcing particles in each nanocomposite was calculated using the Halpin–Tsai model with the measured modulus of the nanocomposites and the unfilled matrix modulus. The modulus of coating films was strongly influenced by the amount of crosslinking; therefore, extra care had been taken to assure the sample films were completely cured in order to avoid changing the modulus of the matrix material without changing the microstructure of the nanocomposite. The Halpin–Tsai model[19–21] can be used as a relatively simple model for determining the aspect ratio of the reinforcing particles. The polydispersity of the reinforcing particles leads to an average particle aspect ratio.

The Halpin–Tsai equation is shown in eq. (3)

$$E_c = E_m \frac{E_f(1 + \varsigma\phi_f) + E_m(\varsigma - \varsigma\phi_f)}{E_f(1 - \phi_f) + E_m(\varsigma + \phi_f)} \quad (3)$$

where E_c is the composite Young's modulus; E_f is the filler modulus; E_m is the matrix modulus; ς is the shape factor, which depends on the geometry, orientation, and aspect ratio of the particles; and ϕ_f is the volume fraction filler.

The shape factors for the tensile moduli of the platelet-reinforced composites are:[22]

1. E_{11} or E_{22} $\varsigma = \frac{2}{3}(w/t)$ in the radial direction of the platelets
2. E_{33} $\varsigma = 2$ perpendicular to the platelets

where (w/t) is the width/thickness of the platelet, which is the aspect ratio.

When the aspect ratios were much smaller than the ratio of filler to matrix modulus ($\varsigma \ll E_f/E_m$), the

Halpin–Tsai model gave results close to those of a series model, whereas if the aspect ratio was much larger than the ratio of filler to matrix modulus ($\varsigma \gg E_f/E_m$), the Halpin–Tsai model gave results close to that of a parallel model. For nanocomposites the series model underestimated the modulus because the volume fraction of filler was very low and thus yielded values close to the matrix modulus. However, the parallel model overestimated the composite modulus at low matrix moduli because it assumed a continuous reinforcing phase. The Halpin–Tsai model [eq. (3)] led to results that were between these two extremes when the aspect ratio was of the same order of magnitude as the ratio of moduli ($\varsigma \approx E_f/E_m$). The aspect ratio of the particles had a strong influence on the results and, therefore, determined how close the results were to either the series or the parallel model. The influence of the aspect ratio and, therefore, also of the level of exfoliation on the modulus was very important. The platelet aspect ratio of layered silicate nanocomposites was typically around 100–200; consequently, when exfoliation was not optimal, the resulting reduction in the effective aspect ratio had a large effect on the modulus. The Halpin–Tsai model can be used to calculate the aspect ratio of the reinforcing particles when the modulus of the composite, matrix, and filler are known. This model only gives an *effective* aspect ratio because the particles can have different shapes, sizes, and thicknesses. The effective aspect ratio represents the best fit with the measured moduli and can be considered a useful parameter to compare different nanocomposite compositions as well as to provide a reasonable estimate of the level of exfoliation achieved.

In the literature, the reinforcement that causes an increase in the modulus when nanofillers are added to polymers is often assumed to be a result of the reduced mobility of a constrained polymer phase close to the silicate layers. The large surface area of the exfoliated platelets is assumed to be responsible for this constrained polymer phase with a higher modulus.[19–21] The increased reinforcement of the whole composite benefits from strong ionic bonds between the polymer and the silicate platelets when more traditional composite models are used.[23] The modulus of the composite is expected to be influenced by the modulus of the matrix, the modulus of the filler, and the shape and orientation of the filler particles.

An increase in modulus was observed over the whole range [see Fig. 6(a)]. The effect was most pronounced above the T_g, with the largest increase occurring at low silicate loadings. The measured matrix modulus of the unfilled system was used in the Halpin–Tsai model to calculate the effective aspect ratios, which were based on particles aligned with their major axes along the test direction, a reasonable assumption from the TEM results. It can be seen in Figure 6(b) that the effective aspect ratio decreased with increasing silicate content, which can be explained by increased stacking at higher silicate loadings. Several studies previously showed reduced exfoliation at a higher silicate content.[24–26] With an increasing concentration, stacking became more pronounced, resulting in an effective aspect ratio that was approximately half the initial value. Although an increase in the modulus below the T_g could be explained by the increasing amount of filler com-

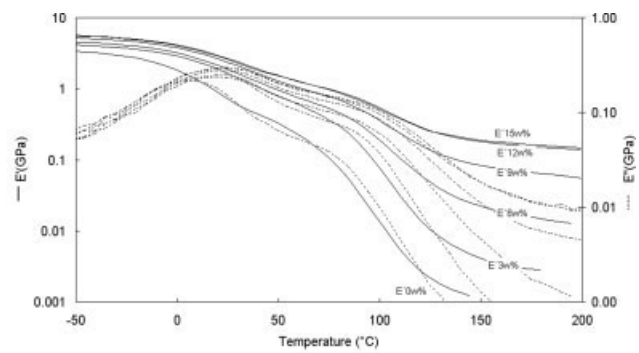

(a)

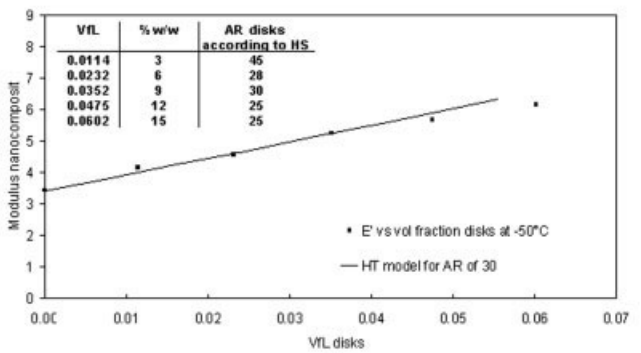

(b)

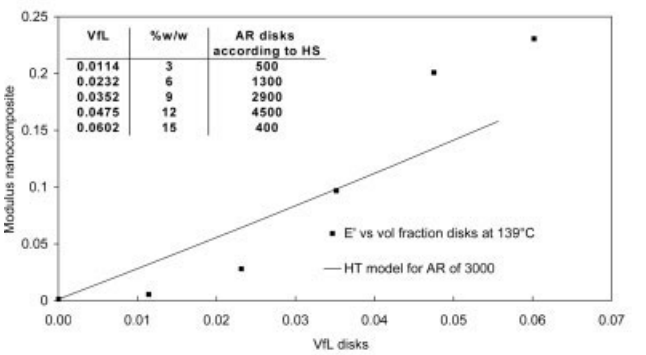

(c)

Figure 6 (a) DTMA data on cured nanocomposite dispersion films containing up to 15% (w/w) laponite particles (b) HT model for moduli observed below the T_g. An aspect ratio of 30 was used for the HT curve (c) HT model for moduli observed above the T_g. An aspect ratio of 3000 was used for the HT curve.

bined with calculation of the effective aspect ratio by the Halpin–Tsai model [see Fig. 6(b)], this method did not account for the enormous increase in modulus above the T_g [see Fig. 6(c)]. The influence of polymer was negligible above the T_g, leaving the influence of the clay network as the most important contribution to the modulus. In this case, calculation of the effective aspect ratio above the T_g yielded impossibly high values. This could be because laponite-coated resin particles in the water phase of the dispersion gave rise to three-dimensional cell structures of laponite when the film was formed. This is partially supported by results of previous studies, as described in the section on analyzing polymer nanocomposite X-ray scattering and shown in Figure 4: depending on the concentration, suspensions of laponite in water form fibrous bundles or more heterogeneous three-dimensional structures.[27] These structures may be trapped between the coalescing resin particles on film formation of the dispersion, giving rise to an enormous increase in modulus above the T_g.

CONCLUSIONS

A route for the preparation of laponite-filled acrylic-based nanocomposite dispersions has been described. This route yielded nanocomposite dispersions in an aqueous environment in whichthe nanoparticles were in the water phase of the dispersion. Various experimental techniques—rheology, X-ray diffraction, DTMA, and TEM—were used to characterize the nanoparticle dispersions and cured films.

DTMA measurement showed a significant improvement in modulus upon the addition of small-aspect-ratio silicate platelets, especially above the T_g of the cured dispersion. The increase in modulus appeared to be more predominant above the T_g as a result of the formation of cell-like structures of individual small laponite disks, as confirmed by TEM measurement. The negligible crosslink density of the polymer system supported this. At the highest concentration of silicate loading, 15% (w/w), the effective aspect ratio was above the T_g (as calculated by HT), similar to the lowest concentration of silicate loading. This is because of the increased number of large three-dimensional structures of laponite disks. It was shown that at higher silicate loadings, the elastic and yield stress behavior of the material became dominant, making the samples more resistant to flow, which was a large disadvantage during processing of the dispersions and hindered leveling during the curing process.

Akzo Nobel Chemicals and Nuplex Resins (previously Akzo Nobel Resins) are kindly acknowledged for providing the resins and for guidance. We acknowledge in particular Dr. Martin Bosma and Mandy van der Horst (AN Chemicals) for the DTMA measurements and Dr. Cees Vijverberg, Dr. Fred van Wijk, and Dr. Andre Roelofs (Nuplex Resins) for all their support. Dr. P. J. Kooyman of the National Center for High Resolution Electron Microscopy, TU Delft, is acknowledged for the TEM analysis. Ben Norder and Gerard de Vos of Polymer and Materials Engineering, TU Delft, are acknowledged for the rheological measurements and TEM sample preparation.

References

1. van Wijk, F. EETK01155 Water Borne Automotive Lakharsen, 2002; available at: www.senternovem.nl.
2. Nobel, M. L.; Picken, S. J.; Mendes, E. Preparation and Properties of Acrylic Based Nanocomposite Resin Coatings; 2006, to appear.
3. Southern Clay Chemicals, 2003; available at: www.nanoclay.com.
4. Rockwood Additives, 2005; available at: www.Laponite.com.
5. Mourchid, A.; Delville, A.; Lambard, J.; LeColier, E.; Levitz, P. Langmuir 1995, 11, 1942.
6. Kroon, M.; Wegdam, G. H.; Sprik, R. Phys Rev 1996, 54, 6.
7. Cousin, F.; Cabuil, V.; Levitz, P. Langmuir 2002, 18, 1466.
8. Training coating technology Module 2; 2002.
9. Bosma, M. Akzo Nobel Chemicals, personal communication; 2005.
10. Vaia, R. A.; Liu, W. J Polym Sci, Part B: Polym Phys 2002, 40, 1590.
11. Roe, R. J. Methods of X-Ray and Neutron Scattering Polymer Science; Oxford University Press: New York, 2000.
12. Mourchid, A.; Delville, A.; Levitz, P. Faraday Discuss 1995, 101, 275.
13. Pignon, F.; Piau, J. M.; Magnin, A. Phys Rev Lett 1996, 76, 4857.
14. Kroon, M.; Vos, W. L.; Wegdam, G. Phys Rev B 1998, E57, 1962.
15. Bonn, D.; Kellay, H.; Tanaka, H.; Wegdam, G.; Meunier, J. Langmuir 1999, 15, 7534.
16. Edwards, A. P.; Bremner, J. J Soil Sci 1967, 18, 64.
17. Olivier, E.; Pefferkorn, E. Colloid Polym Sci 2001, 279, 1104.
18. Giovanini, G.; Sequi, P. Agrochemica 1978, 22, 403.
19. Halpin, J. C.; Kardos, J. L. Polym Eng Sci 1976, 16, 344.
20. Halpin, J. C. J Compos Mater 1969, 3, 732.
21. Yoon, P. J.; Fornes, T. D.; Paul, D. R. Polym Eng Sci 2002, 25, 6727.
22. van Es, M.; Feng, X. Q.; van Turnhout, J.; van der Giessen, E. In Specialty Polymer Additives; Blackwell Science: Oxford, UK, 2001.
23. Shelley, J. S.; Mather, P. T.; DeVries, K. L. Polym Eng Sci 2001, 13, 5849.
24. Liu, L. M.; Qi, Z. N.; Zhu, X. G. J Appl Polym Sci 1999, 71, 1133.
25. van Es, M. Thesis, Delft University of Technology, 2001.
26. Akkapeddi, M. K. Polym Compos 2000, 21, 576.
27. Fornes, T. D.; Paul, D. R. Polym Eng Sci 2003, 17, 4993.